*J. Fluid Mech.* (1987), *vol.* 177, *pp.* 67–82
*Printed in Great Britain*



# An experimental study of the Saffman–Taylor instability

By P. TABELING, G. ZOCCHI AND A. LIBCHABER
The James Franck Institute and E. Fermi Institute,
University of Chicago, 5640 S. Ellis Avenue, Chicago 60615, USA

(Received 14 August 1986)

An experiment on the Saffman–Taylor instability with wetting fluids is presented that explores a greater range of capillary numbers than did the original experiment of Saffman and Taylor. It turns out that no clear one-half plateau for the finger size is observed, and that the ensemble of experiments cannot be analysed in terms of a single control parameter. The effect of the film of oil left behind the finger is important, and we measure its thickness. A qualitative discussion of the instabilities of the fingers for large capillary numbers is presented, the first instability leading to asymmetrical fingers. Tip splitting appears for larger values of $1/B$. The $1/B$ value for the onset of instabilities is shown to be noise dependent.

## 1. Introduction

The penetration of a gas into a viscous fluid in a Hele-Shaw channel (Saffman–Taylor problem) is an example of the general problem of pattern formation in nonlinear systems. In the simplified approach proposed by Saffman & Taylor (1958) in their original paper, the flow of the two fluids is considered to be two dimensional and the interface is a line. In the gas the pressure is uniform, and in the viscous fluid the motion obeys a Darcy law so that all the nonlinearities of the system originate in the boundary conditions at the interface. In the absence of surface tension, a plane interface is unstable at any velocity of propagation. With a finite surface tension, the stability analysis of a flat interface gives a dispersion relation of the form (see e.g. the review paper by Bensimon *et al.* 1986):

$$\omega = \kappa U - \kappa^3 \frac{Tb^2}{12\mu}, \tag{1}$$

where the velocity of the interface $U$ is directed from the air towards the oil, $T$ is the interfacial tension, $\mu$ is the viscosity, $\kappa$ the wavenumber and $\omega$ the exponential growth rate of an initially small sinusoidal disturbance. Since the maximum wavelength allowed by the boundary conditions corresponds to $\kappa_{\min} = 2\pi/w$, where $w$ is the width of the cell, one obtains that the flat interface is unstable if

$$\frac{1}{B} = 12\frac{\mu U}{T}\left(\frac{w}{b}\right)^2 > (2\pi)^2. \tag{2}$$

Experimentally, Saffman & Taylor found that plane interfaces are destabilized by wavelengths scaling approximately with the maximum growth wavelength obtained from (1). The most striking observation was then that the system further evolves towards a state where a single finger occupies about one-half of the channel width at large velocities (figure 1). They could calculate analytically particular steady

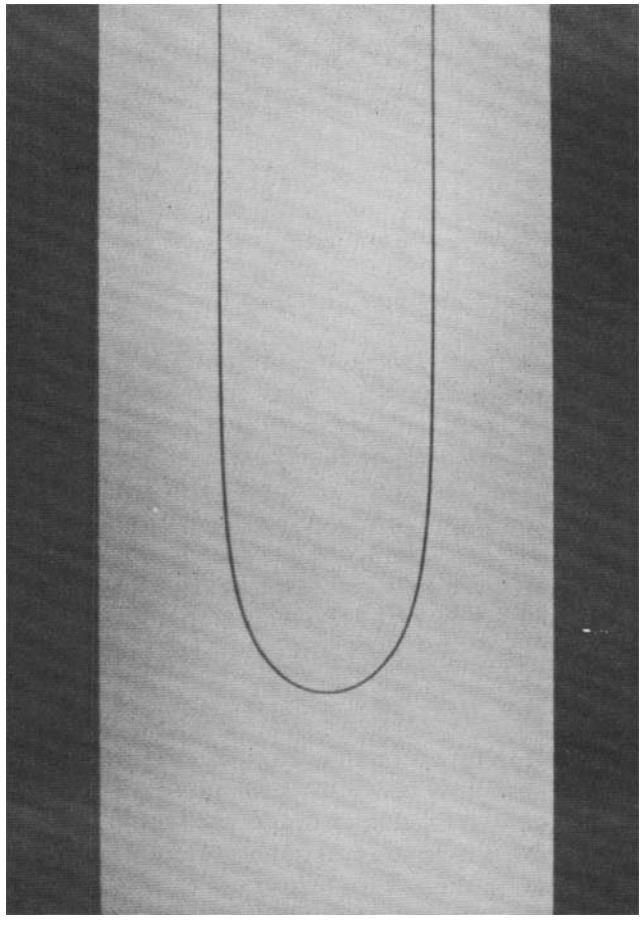

FIGURE 1. Picture of a finger close to $\lambda = \frac{1}{2}$. The dimensions of the cell are: $w = 5.4$ cm and $b = 0.8$ mm. Air penetrating into oil.

solutions of the problem in the zero-surface-tension limit. Using a conformal mapping, they found a continuous family of solutions described by a dimensionless parameter $\lambda$ which represents the relative size of the finger compared to the width of the channel ($0 < \lambda < 1$). The calculated shapes agree very well with the observed ones in the regime of high capillary numbers ($Ca = \mu U/T$), provided that one chooses a value of $\lambda$ equal to the observed one ($\lambda \approx \frac{1}{2}$ in this regime). On the other hand, for small capillary numbers, where surface tension is important, the computed shapes differ substantially from the actual ones.

The problem was reconsidered by McLean & Saffman (1981). Allowing a finite surface tension, they found that $1/B$ defined above is the only parameter that enters the equations of motion. Their numerical study led to values of the size of the finger close to $\frac{1}{2}$ at large velocities, which was in good agreement with the experiments. At low velocities (i.e. $1/B < 100$), the agreement with the experiments was more ambiguous since the finger sizes predicted by the theory were significantly below those actually measured (figure 7).

A more empirical approach to the problem was taken by Pitts (1980). He repeated the experiment of Saffman & Taylor and argued that the flow due to the film left

behind the interface controls the boundary condition on it. He then noticed an intriguing property of self similarity for the shapes of the fingers and built from this experimental fact a theory which gives $\lambda = \frac{1}{2}$ fingers at large velocities. The agreement between theory and experiment was thus obtained at the expense of an empirical assumption.

Another question that is not yet fully understood concerns the mechanism that selects the particular solutions that are observed experimentally. It is known that the McLean–Saffman equations have more than one solution. Romero (1982) found numerically a second set of solutions to these equations, and Vanden-Broeck (1983) showed later that there exists a discrete family of solutions to this problem. On the other hand, only one solution is observed in the experiments.

As for the stability of the fingers, the recent experimental observations (Park & Homsy 1985) and computer simulations (De Gregoria & Schwartz 1985) are that the fingers become unstable at large values of $1/B$, and that the threshold for the onset of the instability depends on the noise. This can be qualitatively understood applying an argument given by Zel'dovitch *et al.* (1980) (Bensimon *et al.* 1986).

The results contained in this paper are the following: since data obtained using cells with different aspect ratios do not fall onto the same curve, a single control parameter like $1/B$ is not enough to describe the system. Also, in experiments with wetting oils no clear $\lambda = \frac{1}{2}$ plateau is observed: the $\lambda$ *vs.* $1/B$ curve shows a slow and continuous decrease below this value for increasing $1/B$. For large values of $1/B$ the fingers become unstable. The first instability that we observe is an asymmetric disturbance on one side of the tip, while at higher velocities tip splitting occurs.

The paper is organized as follows: we first describe the experimental set-up in §2. In §3 we give a description of steady fingers. In §4 we study the low velocity regime. In §5, we study the film left behind the fingers. Then we analyse the large-velocity regime and the stability of the fingers.

## 2. The experimental set-up

Several set-ups have been built for the experiment, but all rely on the same principles. We describe here the last apparatus, from which most of the results presented in this paper have been obtained. The experimental arrangement is sketched in figure 2. The Hele-Shaw cell consists of two long rectangular glass plates separated by two aluminium spacers which define the walls of the channel. The plates are 120 cm long, 10 cm wide and 1.27 cm thick. At either end of the channel are two Plexiglas pieces in which a rectangular cavity the same size as the channel width has been machined in order to limit any possible influence of the extremities of the cell on the flow itself. Those pieces are connected to a hydraulic circuit (composed of valves and a magnetic pump), which in turn is connected to a syphon. The magnetic pump, which was driven by a d.c. motor, was used at large values of the parameter $1/B$. For small values, it turned out to be more convenient to pull the fluid by means of gravitational forces. In both cases, the experimental conditions imposed a constant fluid velocity through the channel. Experiments showed that an accurate control of the velocity was achieved; the regulation was better than $10^{-2}$.

Since the homogeneity of the gap was thought to be a crucial factor for the accuracy of the experimental results (the control parameter $1/B$ depends on $b^2$), we used interferometry to estimate the defects of the cell and eventually reduce them. We found that the inhomogeneity of the gap did not exceed $10^{-3}$ cm throughout the entire channel. The largest non-uniformities were located, as expected, near the ends. In

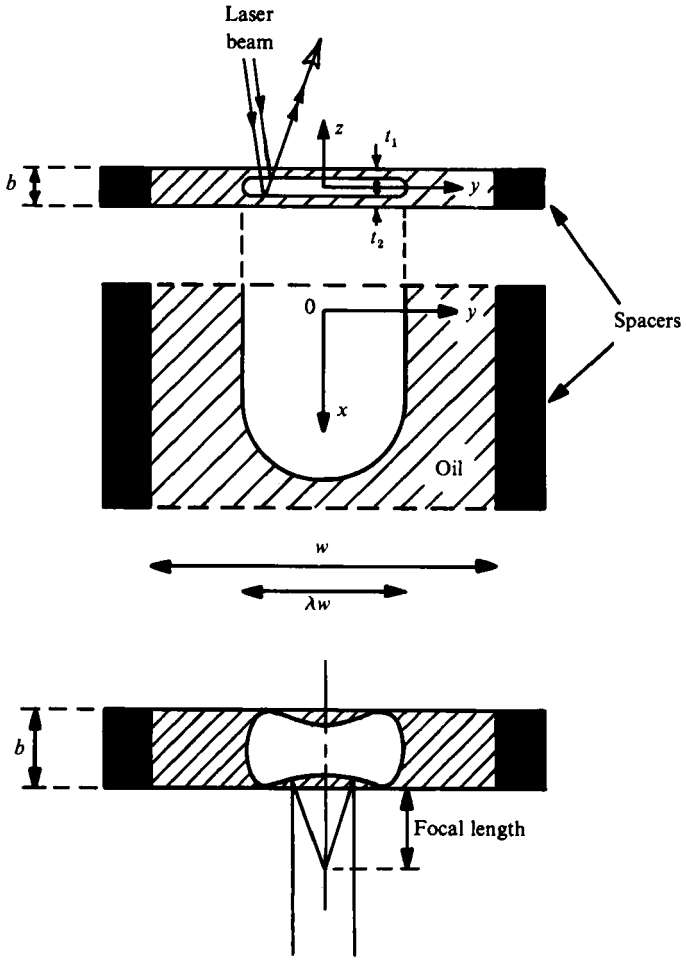


FIGURE 2. Schematic view of the finger and the oil film, which is blown up. The optical beams for the interference study are shown on the top figure. The bottom figure describes how the focal length is measured.

the central part of the cell, the size of the defects lay below $5 \times 10^{-4}$ cm, and it was possible to define a large area for which this value falls to $3 \times 10^{-4}$ cm. These estimates proved to be useful for studying the film left behind the fingers and the fingers' stability.

We chose oils as the viscous fluid in most of the experiments: vacuum pump oil, lubricating oils or silicone oils. Silicone oils Rhodorsil series 47V turned out to be the most convenient because their physical properties are weakly dependent on temperature and they completely wet glass. The test that we used for estimating wetting properties consisted of studying the evolution of the radius of a droplet on a clean surface and comparing it with Tanner's law (1979), which, for a wetting fluid, predicts that the radius will grow as a power of time. Some experiments have been performed with glycerol in order to visualize the flow around the fingers.

The physical parameters of the fluid were measured. The surface tension was determined by three different methods (capillary tube, pendent drop and Padday method 1969), and the viscosity was measured by the falling-ball method.

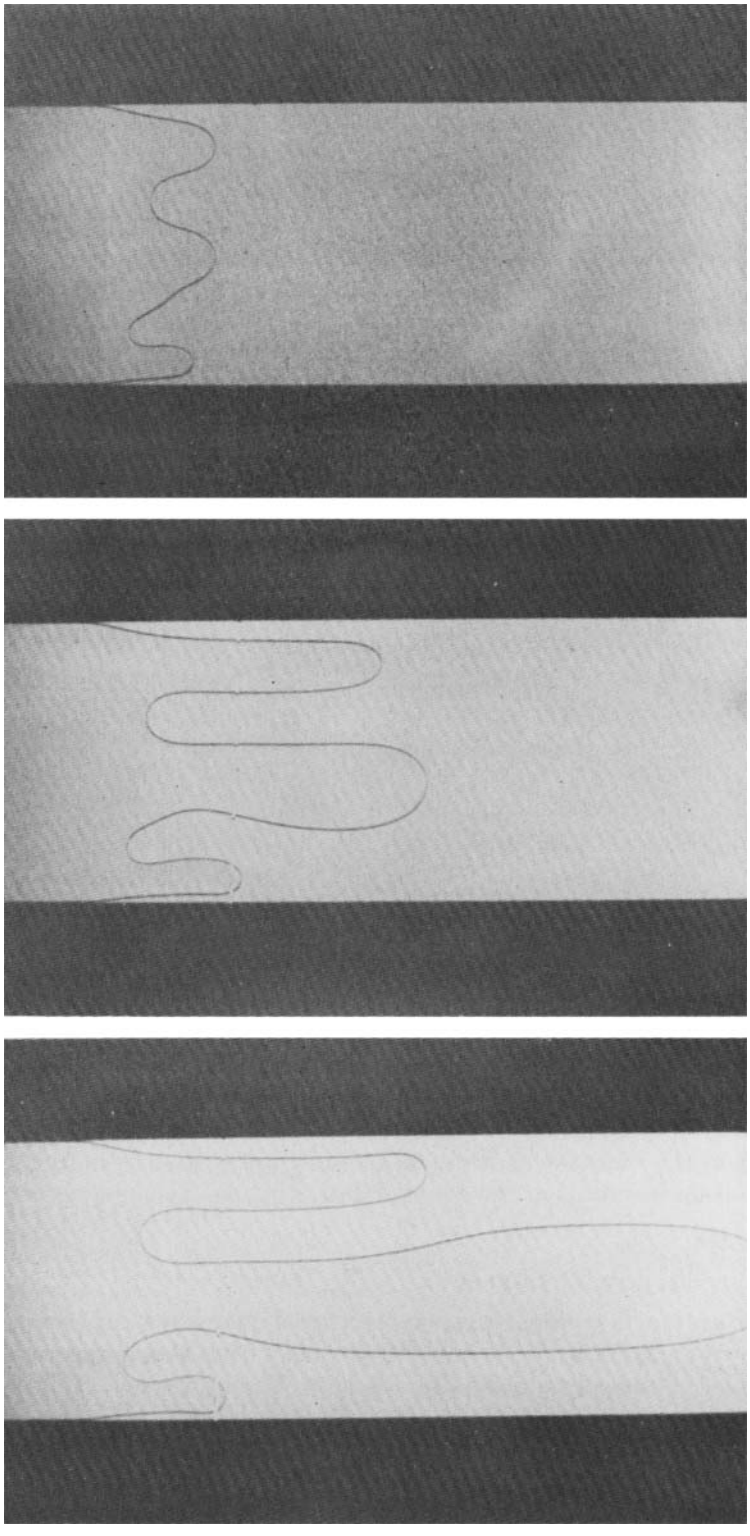

FIGURE 3. Evolution of the transient pattern as a function of time. The bottom figure shows the formation of what will become the stationary finger.

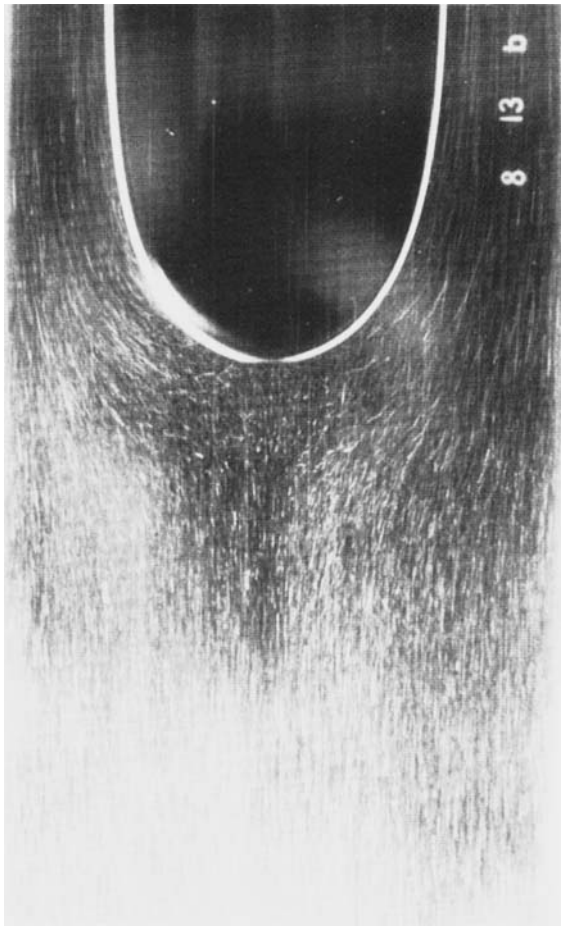


FIGURE 4. Finger of air in glycerol, seeded with small fish-skin particles. Time exposure in the frame of reference of the finger.

Several cells were studied. The gap between the plates was varied by changing the spacers, and the width of the channel could be varied by shifting them. We used three sets of spacers, corresponding to gaps of 800, 480 and 173 μm. In conclusion, we found that the quality of the experiment depends strongly on avoiding pinning effects at the walls and non-uniformities in the channel gap.

## 3. Description of stationary fingers

When an interface starts moving, it generates a few modes which grow and compete together, as shown in figure 3. The competition ends with a single finger occupying a part of the channel and moving steadily along it. The number of modes initially excited depends on the velocity of the interface. Experimentally, we observe that the number of modes increases more or less as the square root of the velocity, as predicted by the linear stability analysis.

An example of a steady finger is shown in figure 1. In the physical space, the dark line, which defines the interface, is a meniscus of oil that scatters the light coming

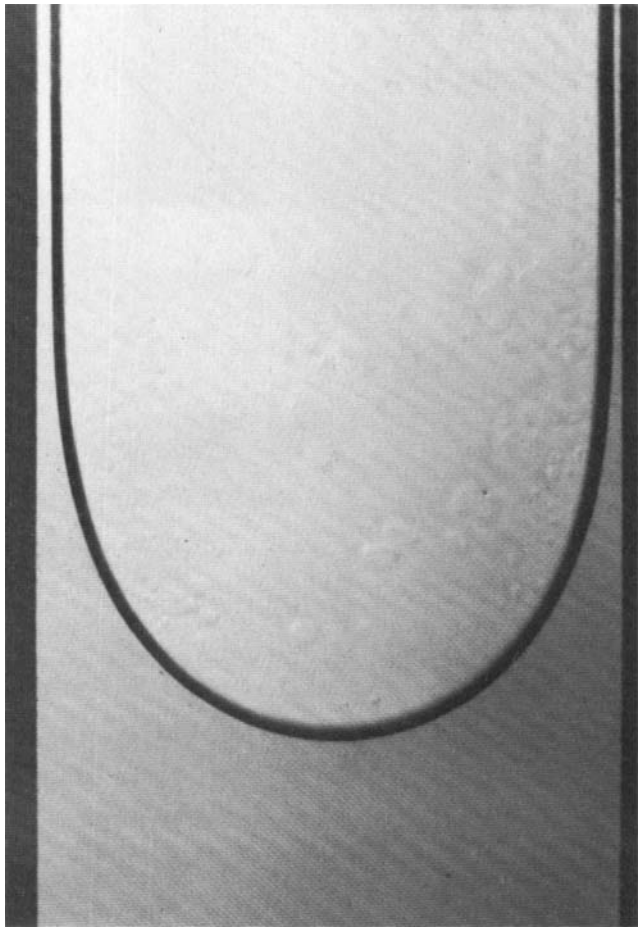

FIGURE 5. Finger shape for $1/B < 50$. At this small velocity one can observe instabilities of the film left behind.

from below. Behind the tip, the interface is parallel to the spacers. One can obtain very long fingers, almost as long as the channel itself.

How is the flow around a steady finger? We have performed experiments with glycerol in order to visualize the motion. Figure 4 shows a time exposure taken in the frame of reference of the finger. The small particles that seed the fluid show two types of trajectories: some of them, originating far ahead, deviate as they approach the finger, and are further convected along its sides. Other particles converge towards the interface, swirl on a small scale as they come close to it, and are further convected backwards. Such motion shows the existence of a pair of small eddies at the tip. Note that a few of them cross the interface and are trapped in the film of glycerine left behind the finger. This motion was previously pointed out by Pitts (1980). An interesting result is the existence of a rolling motion confined in a narrow region close to the interface. This feature has been obtained in a numerical calculation by Reinelt & Saffman (1985), and it shows that in this region the flow is three dimensional. Further away from the tip the streamlines are embedded in horizontal layers and the flow is two dimensional.

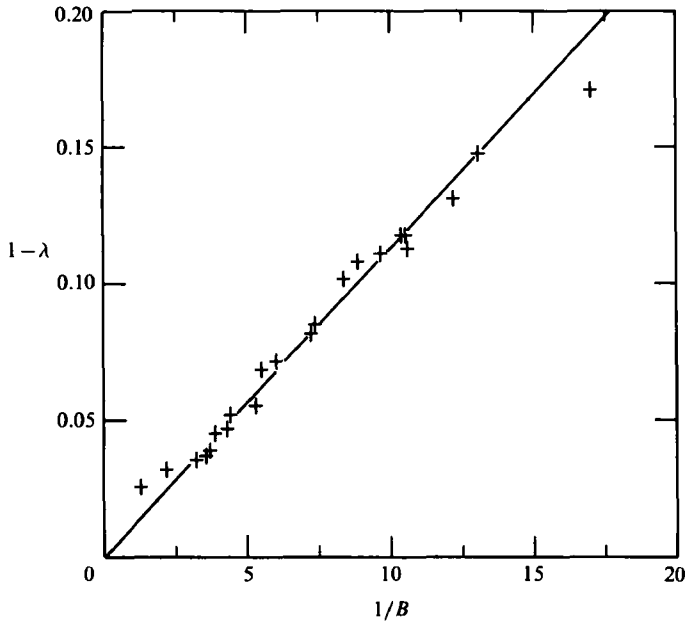


FIGURE 6. Plot of $1-\lambda$ as a function of $1/B$. $w = 3.025$ cm, $b = 0.149$ cm, $\mu = 10$ P, $T = 74$ dynes/cm. High-surface-tension oil is used, and a small-aspect-ratio cell in order to obtain a measurable velocity.

## 4. The low-velocity regime

Phenomenologically, the steady fingers are defined by their velocity $U$, their shape and their size $\lambda$. We now discuss the relation between $\lambda$ and $U$.

The first question that we ask concerns the existence of a control parameter. The relevant pressure terms in the problem are the viscous one, which, using Darcy's law $U = -(b^2/12\mu)\nabla p$ and $w$ as a typical lengthscale, gives $p \approx 12\mu U(w/b^2)$, and the one due to surface tension, which is of order $T/w$, so that we are indeed led to consider the dimensionless number $1/B = 12(w/b)^2\mu(U/T)$ as the control parameter of the system.

Since the size of steady fingers varies rapidly with $1/B$ in the low-velocity regime, we first restrict our study to this region. Experimentally, we observe that the finger shapes become semicircular when the velocity is decreasd to very low values, i.e. for $1/B < 50$ (figure 5). The motion of the fluid around the finger is everywhere as slow as the finger itself and no abnormal draining appears. The finger at rest is not a flat interface because of the influence of the lateral walls; it is a semicircle. Therefore, there seems to be a continuity between the finger at rest and the one moving very slowly.

Physically, it is more natural to characterize the finger sizes by $1-\lambda$, which represents the quantity of fluid left behind the finger as it moves. Our experimental results are presented in figure 6. They show a linear relation between $1-\lambda$ and $1/B$:

$$1-\lambda \approx 0.011/B. \tag{3}$$

This law holds for all values of the aspect ratio $w/b$ measured.

Next we consider larger velocities. Figure 7 summarizes the results that we have obtained for $0 < 1/B < 250$. Experiments have been performed with a large aspect

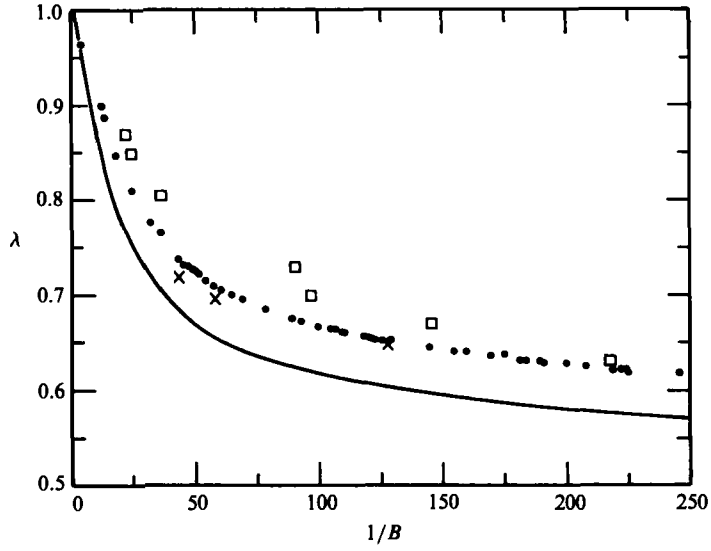


FIGURE 7. Relative size $\lambda$ of the finger as a function of the parameter $1/B$. □, Saffman–Taylor experiment (aspect ratio $w/b = 31.8$); ●, experimental results obtained in cell I, with Rhodorsil oil 47V10; ×, experimental results obtained in a cell of aspect ratio $w/b = 62.3$ with Rhodorsil oil 47V50. Theoretical results of McLean & Saffman are presented as a continuous curve.

ratio $w/b = 65$, and with two oils. The purpose of this experiment was to compare our data with those of Saffman & Taylor, obtained with an aspect ratio about two times smaller.

As shown in figure 7, our data accurately follow a single line which decreases as $1/B$ is increased. The shape of the interface is circular for $1/B < 50$ (figure 5). For larger values of $1/B$ its shape is shown in figure 1. We obtain a result previously shown by Saffman & Taylor: for a given aspect ratio, the curves are universally described by a capillary number, such as $1/B$. As a matter of fact, the data obtained in two closely similar cells but with two different oils lie on a single curve. However, this curve lies significantly below that of Saffman & Taylor. Therefore, we conclude that $1/B$ is not the single control parameter of the problem. We have not found any other parameter for which all the data fit on a single curve. We thus come to the conclusion that the problem is described by two parameters.

If we now look at the theoretical results, we find that they disagree with the two experiments, as shown in figure 7. We therefore suspect that another effect, not taken into account by the theory, is involved in the experiments.

## 5. Influence of the film left behind the fingers

The interface between air and oil is a meniscus which lives in a three-dimensional space. When the interface is advancing, the meniscus produces a film behind it. Basically, this problem is analogous to the Landau–Levich (1942) film drained by a vertical plate. The problem is indeed well defined only when the fluid wets the surface. The theoretical study of the film drained behind a flat interface in a capillary tube has been performed by Bretherton (1961). According to this study, the film thickness follows a $\frac{2}{3}$ power law with the interface velocity, for small velocities; more

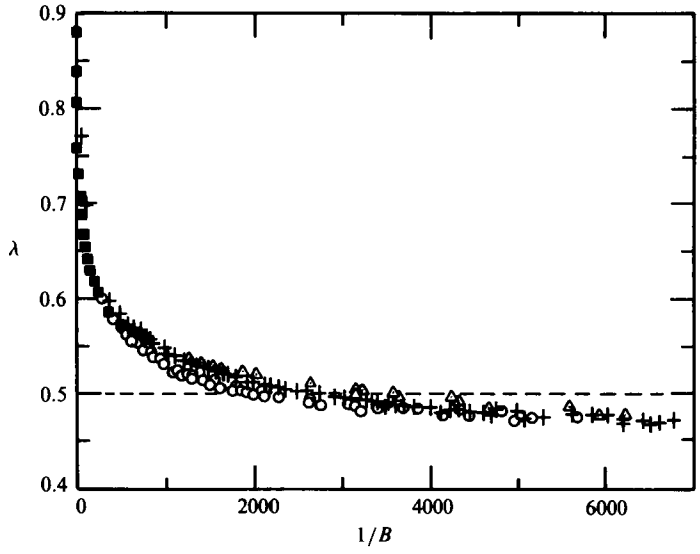


FIGURE 8. Plot of $\lambda$ *vs.* $1/B$ for three different aspect ratios. △, $w/b = 112.5$; +, $w/b = 65$; ○, $w/b = 34$.

precisely, if $R$ is the radius of the capillary tube the formula for the film thickness $t$ reads:

$$\frac{t}{R} = 0.643\,(3Ca)^{\frac{2}{3}}. \tag{4}$$

Accordingly, the pressure drop across the interface is affected by the presence of this film. In general, if the interface is not flat, we expect the film thickness to depend on the velocity component normal to the interface.

When a finger is moving in a Hele-Shaw cell the normal velocity varies along the interface, and therefore one expects the film thickness to be non-uniform behind the interface, which means that the finger moves in a channel of variable gap. Intuitively, one feels that the physical problem may be strongly affected by this phenomenon, and this has been studied theoretically by Park & Homsy (1984).

We performed an experimental study of such a film. The results for low capillary numbers are described in a previous paper by Tabeling & Libchaber (1986). The film thickness was determined interferometrically (figure 2), and it was found that the shape of the film is of the form:

$$t = t_{\max}(U_{\mathrm{n}}/U)^{\frac{2}{3}}, \tag{5}$$

where $U_{\mathrm{n}}$ is the normal velocity. This means that along the interface, the film thickness obeys a local Bretherton law. Also, the maximum thickness $t_{\max}$ as a function of $Ca$ agrees with Bretherton's law for small $Ca$. In this regime the effect of the film on the finger itself can be taken into account by rescaling the parameter $1/B$ using an expression for the pressure drop across the interface derived by Park & Homsy (1984). In this way a better agreement with the McLean–Saffman theory is achieved. We thus find that the film plays a significant role in the experiments and that the previous disagreement between theory and experiments is partly due to the fact that the film had been neglected in the theoretical models.

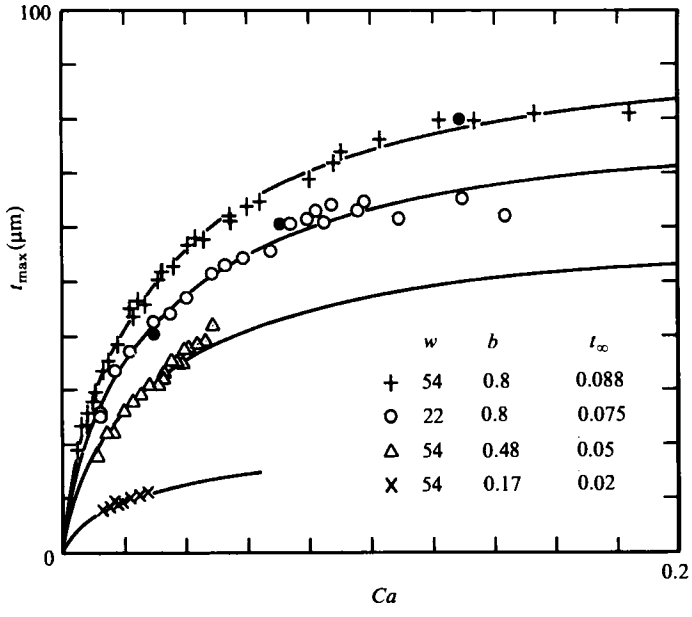


FIGURE 9. Maximum film thickness *vs.* capillary number for various aspect ratios. The solid curves represent the function $t = t_\infty(1 - e^{-\beta Ca^{\frac{1}{2}}})$, with $\beta = 8.585$. ●, numerical results of Reinelt & Saffman. The unit used for $w, b, t_\infty$ is mm.

## 6. The large-velocity regime

For large capillary numbers the experimental results of Saffman & Taylor seemed to indicate that the finger size saturates at the value $\lambda = \frac{1}{2}$. Although this result was also obtained in the numerical analysis of McLean & Saffman, the physical mechanism of such a behaviour remains obscure. We therefore found it useful to get accurate measurements of the finger size for different aspect ratios, in order to define the problem clearly from an experimental point of view. Our results are plotted in figure 8. Different aspect ratios led to slightly different curves. All the curves go below the value $\lambda = \frac{1}{2}$, and the differences between them are small and monotonic with the aspect ratio $w/b$. Hence we do not observe a $\lambda = \frac{1}{2}$ plateau and it appears that $1/B$ is not the only control parameter of the system. Therefore one suspects again that some other physical mechanism, not taken into account by the theory, plays an important role here, evidently related to the evolution of the film thickness in this regime. We thus proceeded to study it.

The interferometric method was difficult to use here, because the growing thickness of the film leads to denser fringes. Therefore we resorted to a different technique, which exploits the fact that the film can be used as a convergent mirror. By measuring its focal length, and inferring its shape from the interferometric measurements at low velocities, we can obtain the maximum thickness $t_{max}$. This analysis presumes that the film shape remains self-similar even at high velocities.

The results obtained for various different cells are shown in figure 9. As is predicted in his paper, Bretherton's law breaks down for values of $Ca$ larger than about $10^{-2}$, and $t_{max}$ saturates at a value which depends on the dimensions of the cell. This technique also enabled us to carry out separate measurements for the top and bottom films, which were indeed found to be symmetric. An experimental study of the film

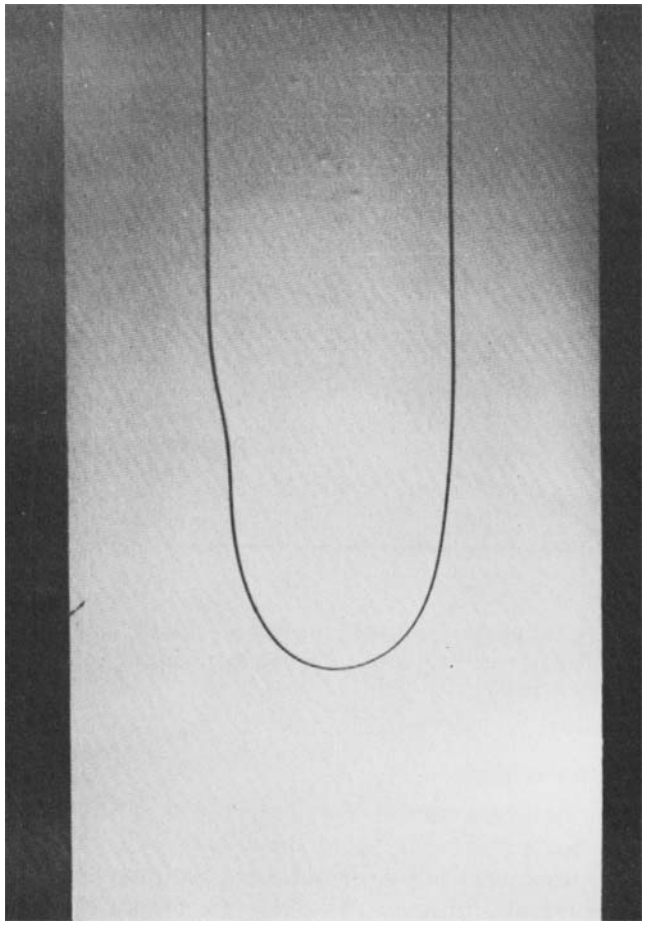

FIGURE 10. Picture of the first instability for $1/B \approx 7000$.

left behind a bubble in a capillary tube was performed by Taylor (1961), and a numerical two-dimensional calculation of the film thickness up to $Ca = 2$ has been published by Reinelt & Saffman (1985). In figure 9 we plot some points taken from figure 4 of that paper, adjusted for a cell thickness of 0.8 mm. When comparing them with the experimental data one has to take into account that in the experiments there is an effect of the aspect ratio on the film thickness, as is apparent from figure 9, while the Reinelt–Saffman calculation corresponds to the limit $w/b \to \infty$.

In passing we note that all the experimental curves can be fitted by a stretched exponential of the form:

$$t_{\max} = \kappa b(1 - e^{-\gamma(w/b)})(1 - e^{-\beta Ca^{\frac{2}{3}}}), \tag{6}$$

with $\kappa \approx 0.119, \gamma \approx 0.038, \beta \approx 8.58$. This law reduces to Bretherton's for small values of $Ca$.

## 7. Study of the stability of the fingers

We have performed several experiments in two different cells in order to study the stability of the fingers.

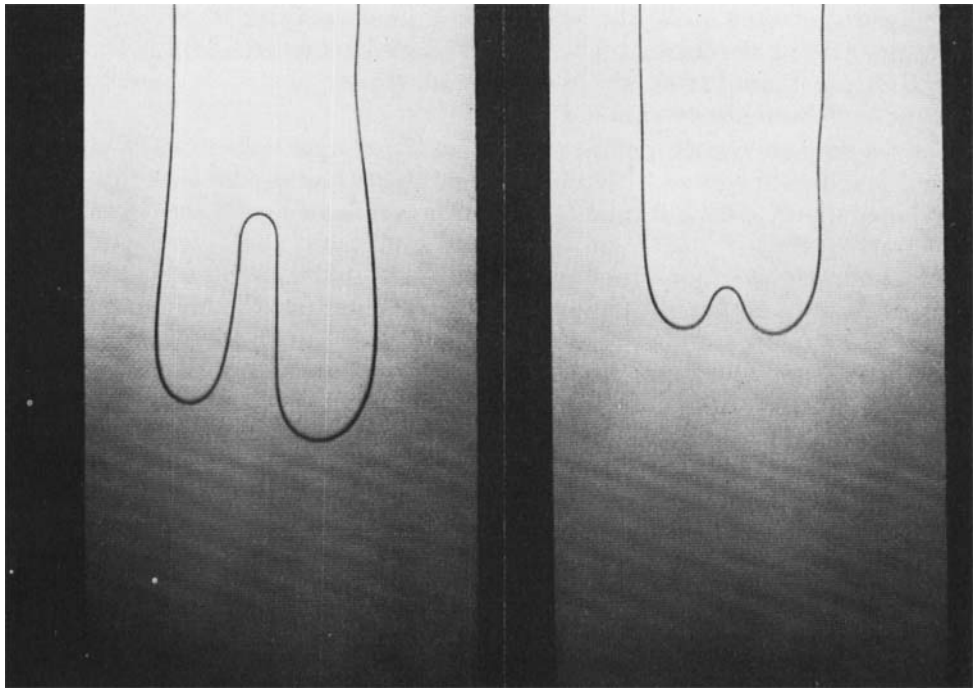

FIGURE 11. Tip splitting instability at two different times.

The first cell (cell I) had dimensions $b = 0.08$ cm, $w = 5.26$ cm and the oil used was Rhodorsil 47V500 ($T = 20.1$ dynes/cm, $\mu = 4.76$ poise). The other cell (cell II) had dimensions $w = 5.7$ cm, $b = 0.076$ cm and the oil used was a lubricating oil, whose characteristics are: $T = 30$ dynes/cm, $\mu = 3$ poises. Both cells have similar characteristics, but the gap of cell II is less uniform than that of cell I: we estimated the maximum variations $\delta b/b$ for cell II equal to $3 \times 10^{-2}$, whereas for cell I it is around $3 \times 10^{-3}$, an order of magnitude improvement in the homogeneity of the gap between the plates. The net result was that for cell II the first instabilities appeared for $1/B \approx 3000$, whereas for cell I the threshold was pushed to $1/B \approx 7000$. Apart from the onset value we have observed the same hierarchy of instabilities for both cells.

Figure 10 shows the first type of disturbance appearing beyond a critical $1/B$ value. When the finger velocity is increased, the interface becomes unstable in the way shown in the figure. A disturbance appears on one side of the tip, grows, recedes backwards and is further damped. In a frame of reference moving with the finger, the disturbance looks like a wave packet which travels backwards, while in the laboratory frame this packet looks stationary. The perturbations are stretched as they move along the interface, as a result of the velocity gradient they encounter. A particular feature of this instability is that it seems to be localized. When a disturbance grows on one side, it leaves the other side unperturbed. There is no real threshold value of $1/B$ for the instability, but in each cell, there is a narrow region in the parameter space above which the fingers are unstable. Let us call it 'threshold region'.

The physical origin of the instability is related to small non-uniformities of the cell as can be surmized from the fact that the disturbances generally appear at the same places in the channel. This feature is clearly observable when $1/B$ is close to the

threshold region. In cell I, when $1/B \approx 7000$, we usually observe one or two disturbances growing along the interface and then decaying for a complete course of the finger along the channel. The number of events increases with $1/B$; for a value of $1/B$ larger than 12000, the disturbances appear almost everywhere; similar features have been observed in cell II.

Beyond the non-symmetric disturbances and for larger values of $1/B$ tip splitting occurs, as shown in figure 11. This kind of instability has also been recently observed experimentally by Park & Homsy (1985) and in computer simulations by De Gregoria & Schwartz (1985).

Let us now try to summarize the theoretical understanding; the puzzling problem was the result of McLean & Saffman (1981) showing that the fingers were linearly unstable. Then came the discovery by De Gregoria & Schwartz (1985), from computer simulations, that noise was an important factor concerning the stability. Then Bensimon (1986), Kessler & Levine (1985) showed that the fingers are linearly stable up to large values of the parameter $1/B$, and they studied the nonlinear instability of the system. There is a strong analogy between the instability of the fingers and that of the premixed flames. The latter problem was analysed by Zel'dovitch *et al.* (1980). In both cases, the non-symmetric disturbances are advected and stretched along the interface. The effect of the advection is stabilizing because the perturbation is brought to regions of lower velocities. The effect of the stretching is also stabilizing because it leads to an increase of the wavelength and hence to a decrease of the amplification rate of the perturbation. The existence of these two mechanisms may explain why the fingers can be stable. Now the instability occurs anyway if the amplitude of the disturbance is large enough. Bensimon *et al.* (1986) have obtained a relation between the amplitude of the noise $\nu_c$ necessary to obtain marginal eigenvalues and the parameter $1/B$. The striking result is that $\nu_c$ is an exponential function of $1/B$, so that the instability threshold is entirely determined by the velocity. The picture that they obtained is that of a system extremely sensitive to changes in velocity as far as the stability is concerned.

From the experimental side, many observed features are in agreement with the theory. The description of the evolution of the non-symmetric disturbances is very close to that predicted by the theory; also the shapes of the unstable fingers are in excellent agreement with the theory (see Bensimon (1986) in which a detailed comparison is made).

However, the agreement becomes more ambiguous when we look at the sensitivity of the system to noise. According to the theory, the instability of the fingers is controlled by $1/B$: significant differences between the intrinsic noise of two experiments should induce only small changes for the 'threshold' value of $1/B$. This is not what we observe. Small improvements of the quality of our experimental set-up led to dramatic changes in the threshold values of $1/B$, while the threshold value itself is not sharply defined.

We have tried to go further into this question by applying some external perturbation on the interfaces and see how they eventually become unstable. The perturbation was an electric field. Although such experiments were not entirely conclusive, it appeared that the critical value of the noise was weakly dependent on the velocity below the threshold region, which is in conflict with theory.

The origin of such a disagreement is possibly related to the existence of the film, which has been neglected by the theory. The effect of the film is stabilizing. For the case of a plane interface, the analysis shows that the presence of a film reduces the amplification rate of the disturbance and shifts the critical wavenumber towards

smaller values. One feels that both effects can play a role in the nonlinear stability of the fingers.

## 8. Conclusion

The main conclusion of this paper is that the film plays a crucial role in the Saffman–Taylor problem. This was realized by Pitts (1980) and by McLean & Saffman, and the Reinelt–Saffman work was stimulated by this question, but no clear experimental account of its importance has been reported previously. We do not observe a $\lambda = \frac{1}{2}$ plateau in the $\lambda$ *vs.* $1/B$ curve for large $1/B$, and this can be ascribed to the fact that the curvature of the meniscus keeps changing with changing $Ca$. Concerning the stability of the fingers, we observe that the value of $1/B$ at which the first instabilities occur depend strongly on the noise.

We thank D. Bensimon, M. Jensen, L. Kadanoff and P. Pelcé for very illuminating discussions. This work was supported by the National Science Foundation under Grant N. DMR-8316204, and also by an NSFINT-8412371 exchange award for P. Tabeling.

## REFERENCES

Bensimon, D. 1986 Stability of viscous fingering. *Phys. Rev.* A (in press).

Bensimon, D., Kadanoff, L. P., Liang, S., Shraiman, B. I. & Tang, C. 1986 Viscous flows in two dimensions. *Rev. Mod. Phys.* (in press).

Bretherton, F. P. 1961 The motion of long bubbles in tubes. *J. Fluid Mech.* **10**, 166.

De Gregoria, A. J. & Schwartz, L. W. 1985 A boundary integral method for two-phase displacement in Hele-Shaw cells. *Exxon preprints.*

Hele-Shaw, H. J. S. 1898 On the motion of a viscous fluid between two parallel plates. *Nature* **58**, 34.

Kessler, D. A. & Levine, H. 1985 Theory of the Saffman–Taylor finger. Preprint.

Landau, L. & Levich, B. 1942 Dragging of a liquid by a moving plate. *Acta Phisicochimica USSR* **17**, 42.

McLean, J. W. 1980 The fingering problem in flows through porous media. PhD thesis, Caltech.

McLean, J. W. & Saffman, P. G. 1981 The effect of surface tension on the shape of fingers in a Hele-Shaw cell. *J. Fluid Mech.* **102**, 455.

Maher, J. 1985 The development of viscous fingering patterns. *Phys. Rev. Lett.* **54**, 1498.

Padday, J. F. 1969 In *Surface and Colloid Science* (ed. E. Matijevic), vol. 1, p. 39. Wiley.

Park, C. W., Gorell, S. & Homsy, G. M. 1984 Two-phase displacement in Hele-Shaw cells: experiments on viscously driven instabilities. *J. Fluid Mech.* **141**, 275.

Park, C. W. & Homsy, G. M. 1984 Two phase displacement in Hele-Shaw cells: theory. *J. Fluid Mech.* **139**, 291.

Park, C. W. & Homsy, G. M. 1985 The instability of long fingers in Hele-Shaw flows. *Phys. Fluids* **28**, 1583.

Pitts, E. 1980 Penetration of fluids into a Hele-Shaw cell. *J. Fluid Mech.* **97**, 53.

Reinelt, D. A. & Saffman, P. G. 1985 The penetration of a finger into a viscous fluid in a channel and tube. *J. Sci. Stat. Comput.* **6** (3), 542.

Romero, L. 1982 PhD thesis. California Institute of Technology.

Saffman, P. G. & Taylor, G. I. 1958 The penetration of a fluid into a porous medium or Hele-Shaw cell containing a more viscous liquid. *Proc. R. Soc. Lond.* A **245**, 312.

Shraiman, B. I. & Bensimon, D. 1984 Singularities in non local interface dynamics. *Phys. Rev.* A **30**, 2840.

TABELING, P. & LIBCHABER, A. 1986 Film draining and the Saffman–Taylor problem. *Phys. Rev.* A **33**, 794.

TANNER, L. H. 1979 The spreading of silicone oil drops on horizontal surfaces. *J. Phys.* D: *Appl. Phys.* **12**, 1473.

TAYLOR, G. I. 1961 Deposition of a viscous fluid on the wall of a tube. *J. Fluid Mech.* **10**, 161.

VANDEN-BROECK, J.-M. 1983 Fingers in Hele-Shaw cells with surface tension. *Phys. Fluids* **26**, 2033.

ZEL'DOVITCH, YA. B., ISTRATOV, A. G., KIDIN, N. I. & LIBROVITCH, V. B. 1980 Flame propagation in tubes: hydrodynamics and stability. *Comb. Sci. Tech.* **24**, 1.